

## Measurement of the $D_s^+ \rightarrow \eta \ell^+ \nu$ and $D_s^+ \rightarrow \eta' \ell^+ \nu$ Branching Ratios

G. Brandenburg,<sup>1</sup> D. Cinabro,<sup>1</sup> T. Liu,<sup>1</sup> M. Saulnier,<sup>1</sup> R. Wilson,<sup>1</sup> H. Yamamoto,<sup>1</sup> T. Bergfeld,<sup>2</sup>  
 B. I. Eisenstein,<sup>2</sup> J. Ernst,<sup>2</sup> G. E. Gladding,<sup>2</sup> G. D. Gollin,<sup>2</sup> M. Palmer,<sup>2</sup> M. Selen,<sup>2</sup> J. J. Thaler,<sup>2</sup> K. W. Edwards,<sup>3</sup>  
 K. W. McLean,<sup>3</sup> M. Ogg,<sup>3</sup> A. Bellerive,<sup>4</sup> D. I. Britton,<sup>4</sup> E. R. F. Hyatt,<sup>4</sup> R. Janicek,<sup>4</sup> D. B. MacFarlane,<sup>4</sup> P. M. Patel,<sup>4</sup>  
 B. Spaan,<sup>4</sup> A. J. Sadoff,<sup>5</sup> R. Ammar,<sup>6</sup> P. Baringer,<sup>6</sup> A. Bean,<sup>6</sup> D. Besson,<sup>6</sup> D. Coppage,<sup>6</sup> N. Copty,<sup>6</sup> R. Davis,<sup>6</sup>  
 N. Hancock,<sup>6</sup> S. Kotov,<sup>6</sup> I. Kravchenko,<sup>6</sup> N. Kwak,<sup>6</sup> Y. Kubota,<sup>7</sup> M. Lattery,<sup>7</sup> M. Momayezi,<sup>7</sup> J. K. Nelson,<sup>7</sup>  
 S. Patton,<sup>7</sup> R. Poling,<sup>7</sup> V. Savinov,<sup>7</sup> S. Schrenk,<sup>7</sup> R. Wang,<sup>7</sup> M. S. Alam,<sup>8</sup> I. J. Kim,<sup>8</sup> Z. Ling,<sup>8</sup> A. H. Mahmood,<sup>8</sup>  
 J. J. O'Neill,<sup>8</sup> H. Severini,<sup>8</sup> C. R. Sun,<sup>8</sup> F. Wappler,<sup>8</sup> G. Crawford,<sup>9</sup> J. E. Duboscq,<sup>9</sup> R. Fulton,<sup>9</sup> D. Fujino,<sup>9</sup> K. K. Gan,<sup>9</sup>  
 K. Honscheid,<sup>9</sup> H. Kagan,<sup>9</sup> R. Kass,<sup>9</sup> J. Lee,<sup>9</sup> M. Sung,<sup>9</sup> C. White,<sup>9</sup> A. Wolf,<sup>9</sup> M. M. Zoeller,<sup>9</sup> X. Fu,<sup>10</sup> B. Nemat,<sup>10</sup>  
 W. R. Ross,<sup>10</sup> P. Skubic,<sup>10</sup> M. Wood,<sup>10</sup> M. Bishai,<sup>11</sup> J. Fast,<sup>11</sup> E. Gerndt,<sup>11</sup> J. W. Hinson,<sup>11</sup> T. Miao,<sup>11</sup> D. H. Miller,<sup>11</sup>  
 M. Modesitt,<sup>11</sup> E. I. Shibata,<sup>11</sup> I. P. J. Shipsey,<sup>11</sup> P. N. Wang,<sup>11</sup> L. Gibbons,<sup>12</sup> S. D. Johnson,<sup>12</sup> Y. Kwon,<sup>12</sup> S. Roberts,<sup>12</sup>  
 E. H. Thorndike,<sup>12</sup> T. E. Coan,<sup>13</sup> J. Dominick,<sup>13</sup> V. Fadeyev,<sup>13</sup> I. Korolkov,<sup>13</sup> M. Lambrecht,<sup>13</sup> S. Sanghera,<sup>13</sup>  
 V. Shelkov,<sup>13</sup> T. Skwarnicki,<sup>13</sup> R. Stroynowski,<sup>13</sup> I. Volobouev,<sup>13</sup> G. Wei,<sup>13</sup> M. Artuso,<sup>14</sup> M. Gao,<sup>14</sup> M. Goldberg,<sup>14</sup>  
 D. He,<sup>14</sup> N. Horwitz,<sup>14</sup> S. Kopp,<sup>14</sup> G. C. Moneti,<sup>14</sup> R. Mountain,<sup>14</sup> F. Muheim,<sup>14</sup> Y. Mukhin,<sup>14</sup> S. Playfer,<sup>14</sup> S. Stone,<sup>14</sup>  
 X. Xing,<sup>14</sup> J. Bartelt,<sup>15</sup> S. E. Csorna,<sup>15</sup> V. Jain,<sup>15</sup> S. Marka,<sup>15</sup> D. Gibaut,<sup>16</sup> K. Kinoshita,<sup>16</sup> P. Pomianowski,<sup>16</sup>  
 B. Barish,<sup>17</sup> M. Chadha,<sup>17</sup> S. Chan,<sup>17</sup> D. F. Cowen,<sup>17</sup> G. Eigen,<sup>17</sup> J. S. Miller,<sup>17</sup> C. O'Grady,<sup>17</sup> J. Urheim,<sup>17</sup>  
 A. J. Weinstein,<sup>17</sup> F. Würthwein,<sup>17</sup> D. M. Asner,<sup>18</sup> M. Athanas,<sup>18</sup> D. W. Bliss,<sup>18</sup> W. S. Brower,<sup>18</sup> G. Masek,<sup>18</sup>  
 H. P. Paar,<sup>18</sup> J. Gronberg,<sup>19</sup> C. M. Korte,<sup>19</sup> R. Kutschke,<sup>19</sup> S. Menary,<sup>19</sup> R. J. Morrison,<sup>19</sup> S. Nakanishi,<sup>19</sup>  
 H. N. Nelson,<sup>19</sup> T. K. Nelson,<sup>19</sup> C. Qiao,<sup>19</sup> J. D. Richman,<sup>19</sup> D. Roberts,<sup>19</sup> A. Ryd,<sup>19</sup> H. Tajima,<sup>19</sup> M. S. Witherell,<sup>19</sup>  
 R. Balest,<sup>20</sup> K. Cho,<sup>20</sup> W. T. Ford,<sup>20</sup> M. Lohner,<sup>20</sup> H. Park,<sup>20</sup> P. Rankin,<sup>20</sup> J. G. Smith,<sup>20</sup> J. P. Alexander,<sup>21</sup>  
 C. Bebek,<sup>21</sup> B. E. Berger,<sup>21</sup> K. Berkelman,<sup>21</sup> K. Bloom,<sup>21</sup> T. E. Browder,<sup>21,\*</sup> D. G. Cassel,<sup>21</sup> H. A. Cho,<sup>21</sup>  
 D. M. Coffman,<sup>21</sup> D. S. Crowcroft,<sup>21</sup> M. Dickson,<sup>21</sup> P. S. Drell,<sup>21</sup> D. J. Dumas,<sup>21</sup> R. Ehrlich,<sup>21</sup> R. Elia,<sup>21</sup> P. Gaidarev,<sup>21</sup>  
 M. Garcia-Sciveres,<sup>21</sup> B. Gittelman,<sup>21</sup> S. W. Gray,<sup>21</sup> D. L. Hartill,<sup>21</sup> B. K. Heltsley,<sup>21</sup> S. Henderson,<sup>21</sup> C. D. Jones,<sup>21</sup>  
 S. L. Jones,<sup>21</sup> J. Kandaswamy,<sup>21</sup> N. Katayama,<sup>21</sup> P. C. Kim,<sup>21</sup> D. L. Kreinick,<sup>21</sup> T. Lee,<sup>21</sup> Y. Liu,<sup>21</sup> G. S. Ludwig,<sup>21</sup>  
 J. Masui,<sup>21</sup> J. Mevissen,<sup>21</sup> N. B. Mistry,<sup>21</sup> C. R. Ng,<sup>21</sup> E. Nordberg,<sup>21</sup> J. R. Patterson,<sup>21</sup> D. Peterson,<sup>21</sup> D. Riley,<sup>21</sup>  
 A. Soffer,<sup>21</sup> P. Avery,<sup>22</sup> A. Freyberger,<sup>22</sup> K. Lingel,<sup>22</sup> C. Prescott,<sup>22</sup> J. Rodriguez,<sup>22</sup> S. Yang,<sup>22</sup> and J. Yelton<sup>22</sup>

(CLEO Collaboration)

<sup>1</sup>Harvard University, Cambridge, Massachusetts 02138

<sup>2</sup>University of Illinois, Champaign-Urbana, Illinois 61801

<sup>3</sup>Carleton University, Ottawa, Ontario, Canada K1S 5B6  
and the Institute of Particle Physics, Montreal, Canada

<sup>4</sup>McGill University, Montréal, Québec, Canada H3A 2T8  
and the Institute of Particle Physics, Montreal, Canada

<sup>5</sup>Ithaca College, Ithaca, New York 14850

<sup>6</sup>University of Kansas, Lawrence, Kansas 66045

<sup>7</sup>University of Minnesota, Minneapolis, Minnesota 55455

<sup>8</sup>State University of New York at Albany, Albany, New York 12222

<sup>9</sup>Ohio State University, Columbus, Ohio 43210

<sup>10</sup>University of Oklahoma, Norman, Oklahoma 73019

<sup>11</sup>Purdue University, West Lafayette, Indiana 47907

<sup>12</sup>University of Rochester, Rochester, New York 14627

<sup>13</sup>Southern Methodist University, Dallas, Texas 75275

<sup>14</sup>Syracuse University, Syracuse, New York 13244

<sup>15</sup>Vanderbilt University, Nashville, Tennessee 37235

<sup>16</sup>Virginia Polytechnic Institute and State University, Blacksburg, Virginia 24061

<sup>17</sup>California Institute of Technology, Pasadena, California 91125

<sup>18</sup>University of California, San Diego, La Jolla, California 92093

<sup>19</sup>University of California, Santa Barbara, California 93106

<sup>20</sup>University of Colorado, Boulder, Colorado 80309-0390

<sup>21</sup>Cornell University, Ithaca, New York 14853

<sup>22</sup>University of Florida, Gainesville, Florida 32611

(Received 24 July 1995)

Using the CLEO II detector we measure  $\mathcal{B}(D_s^+ \rightarrow \eta e^+ \nu)/\mathcal{B}(D_s^+ \rightarrow \phi e^+ \nu) = 1.24 \pm 0.12 \pm 0.15$ ,  $\mathcal{B}(D_s^+ \rightarrow \eta' e^+ \nu)/\mathcal{B}(D_s^+ \rightarrow \phi e^+ \nu) = 0.43 \pm 0.11 \pm 0.07$ , and  $\mathcal{B}(D_s^+ \rightarrow \eta' e^+ \nu)/\mathcal{B}(D_s^+ \rightarrow \eta e^+ \nu) = 0.35 \pm 0.09 \pm 0.07$ . We find the ratio of vector to pseudoscalar final states,  $\mathcal{B}(D_s^+ \rightarrow \phi e^+ \nu)/\mathcal{B}(D_s^+ \rightarrow (\eta + \eta') e^+ \nu) = 0.60 \pm 0.06 \pm 0.06$ , which is similar to the ratio found in nonstrange  $D$  decays.

PACS numbers: 13.20.Fc, 13.65.+i, 14.40.Lb

One of the outstanding problems in charm semileptonic decay is the difficulty in computing the ratio of vector to pseudoscalar final states,  $\mathcal{B}(D \rightarrow \bar{K}^* \ell^+ \nu)/\mathcal{B}(D \rightarrow \bar{K} \ell^+ \nu)$ . The experimental average for this ratio is  $0.56 \pm 0.06$  [1], while theoretical predictions range from 0.5 to 1.2 [1,2]. It is important to repeat these measurements for the  $D_s^+$ , where the initial and final hadrons differ by the substitution of a light quark by a strange quark. In the  $D_s^+$  sector only the  $D_s^+ \rightarrow \phi \ell^+ \nu$  decay has been extensively studied. The Fermilab experiment E653 has seen evidence for the remaining major  $D_s^+$  semileptonic modes,  $D_s^+ \rightarrow (\eta + \eta') \mu^+ \nu$  [3]. In this paper we report the first measurements of  $\mathcal{B}(D_s^+ \rightarrow \eta \ell^+ \nu)$  and  $\mathcal{B}(D_s^+ \rightarrow \eta' \ell^+ \nu)$  and determine the vector to pseudoscalar ratio. The data include events with both muons and electrons.

The data consist of an integrated luminosity of  $3.11 \text{ fb}^{-1}$  of  $e^+e^-$  collisions recorded with the CLEO II detector at the Cornell Electron Storage Ring (CESR). The data sample contains about  $3.7 \times 10^6 e^+e^- \rightarrow c\bar{c}$  events taken at center-of-mass energies on the  $Y(4S)$  resonance and in the nearby continuum. The CLEO II detector includes a CsI electromagnetic calorimeter that provides excellent  $\eta$  reconstruction [4].

Because of the undetected neutrino, we cannot fully reconstruct  $D_s^+ \rightarrow X \ell^+ \nu$  decays, where  $X \equiv \phi, \eta, \text{ or } \eta'$  and  $\ell^+ \equiv e^+ \text{ or } \mu^+$ . However, there are few processes which produce both a meson  $X$  and a lepton in the same jet. This correlation is used to extract a clean  $D_s^+ \rightarrow X \ell^+ \nu$  signal by requiring that  $X$  and the lepton be in the same hemisphere with respect to the thrust axis of the event. Backgrounds can be reduced for  $D_s^+ \rightarrow \eta \ell^+ \nu$  and  $D_s^+ \rightarrow \phi \ell^+ \nu$ , which have sufficient statistics, by also detecting the low energy photon from the  $D_s^{*+} \rightarrow D_s^+ \gamma$  decay. We refer to this second method as the  $D_s^{*+}$  tag analysis.

Electron and muon candidates are restricted to lie in the fiducial regions  $|\cos\theta| < 0.91$  and  $|\cos\theta| < 0.81$ , respectively, where  $\theta$  is the polar angle of the track with respect to the beam axis. Electron candidates are required to have momenta above 0.7 and 1.0 GeV/ $c$  for the  $D_s^{*+}$  tag and nontag analyses, respectively. Electrons are identified by comparing their ionization energy loss, time of flight, energy deposit, and shower shapes in the electromagnetic calorimeter with that expected for true electrons. Electrons from photon conversions and Dalitz decays of  $\pi^0$ 's are rejected. Muon candidate tracks in the region  $|\cos\theta| < 0.61$  ( $|\cos\theta| > 0.61$ ) are required to have momenta above 1.5 GeV/ $c$  (1.9 GeV/ $c$ ) and must penetrate at least 5 interaction lengths of iron.

We identify  $\phi, \eta, \text{ and } \eta'$  candidates by detecting decays to  $K^+K^-, \gamma\gamma, \text{ and } \eta\pi^+\pi^-$ , respectively. We require that the momenta of these states be greater than 1.0 GeV/ $c$  to reduce combinatoric background. Charged kaon (pion) candidates are required to have ionization energy loss and time of flight consistent with that expected for true kaons (pions). Momentum dependent efficiencies for identifying kaons in  $\phi$  decays are obtained from the data by comparing the inclusive  $\phi$  yield before and after particle identification. These efficiencies are then combined with the predicted  $\phi$  momentum spectrum from  $D_s^+ \rightarrow \phi \ell^+ \nu$  Monte Carlo events to give the total  $\phi$  identification efficiency. Photon candidates must lie in the fiducial region  $|\cos\theta| < 0.81$  and have a lateral shower shape consistent with that expected for photons. In reconstructing the  $\eta$  we require  $|\cos\theta_d| < 0.9$  to reduce random combinations of low momentum photons, where  $\theta_d$  is the photon decay angle in the  $\eta$  rest frame with respect to the  $\eta$  direction in the laboratory. We veto any photon which, when combined with another photon, has an invariant mass consistent with the  $\pi^0$  mass and a momentum greater than 0.8 GeV/ $c$ . In reconstructing the  $\eta'$  we require that the invariant mass of the two photons from  $\eta \rightarrow \gamma\gamma$  decays be consistent with the  $\eta$  mass and that the  $\eta$  momentum be greater than 0.5 GeV/ $c$ . Pion identification efficiency in  $\eta'$  decays is obtained from the inclusive  $\eta'$  data in the same manner as the kaon identification efficiency for  $\phi$  reconstruction.

To suppress combinatoric background from the more spherical  $Y(4S)$  events we require that the ratio of Fox-Wolfram moments [5],  $H_2/H_0$ , be greater than 0.30. The  $X$  candidates are combined with a lepton, and the  $X\ell^+$  combinations must have an invariant mass less than 1.9 GeV/ $c^2$ . For  $\eta\ell^+$  candidates we require that the  $\eta\ell^+$  invariant mass be greater than 1.2 GeV/ $c^2$ ; the  $X\ell^+$  momentum must be less than 4.5 GeV/ $c$  and greater than 2.0 and 2.5 GeV/ $c$  for the  $D_s^{*+}$  tag and nontag analyses, respectively. All kinematic requirements on the lepton,  $X$ , and  $X\ell^+$  candidates are determined from the Monte Carlo simulation to reduce combinatoric backgrounds. The  $K^+K^-, \gamma\gamma, \text{ and } \eta\pi^+\pi^-$  invariant mass spectra for all  $X\ell^+$  combinations which pass the above selection criteria are fit to obtain the number of candidates which are given in Table I. Figures 1(a) and 1(b) show the invariant mass spectra for  $\gamma\gamma$  and  $\eta\pi^+\pi^-$ . Efficiencies are determined using Monte Carlo events (generated according to the ISGW model [6]) and processed through a full simulation of the CLEO II detector and the same event reconstruction and analysis chain as the data.

TABLE I. Summary of the  $D_s^{*+}$  nontag and tag analyses for the sum of events with  $e^+$  and  $\mu^+$ . The errors quoted in this table are statistical only.

Decay mode	$D_s^{*+}$ nontag			$D_s^{*+}$ tag	
	$D_s^+ \rightarrow \phi \ell^+ \nu$	$D_s^{*+} \rightarrow \eta \ell^+ \nu$	$D_s^+ \rightarrow \eta' \ell^+ \nu$	$D_s^+ \rightarrow \phi \ell^+ \nu$	$D_s^+ \rightarrow \eta \ell^+ \nu$
Candidates	$863.6 \pm 40.5$	$577.6 \pm 30.3$	$42.3 \pm 7.9$	$326.9 \pm 27.1$	$153.4 \pm 15.0$
Fake lepton	$95.3 \pm 2.2$	$128.8 \pm 1.6$	$9.0 \pm 0.4$	$27.9 \pm 1.2$	$22.7 \pm 0.7$
Continuum bkgd.	$23.1 \pm 0.8$	$35.1 \pm 2.0$	$0.0 \pm 0.0$	$15.6 \pm 0.7$	$8.5 \pm 1.0$
$B\bar{B}$ bkgd.	$49.6 \pm 1.8$	$27.6 \pm 2.5$	$1.9 \pm 0.2$	$7.9 \pm 0.7$	$3.8 \pm 1.0$
$D_s^+ \rightarrow \eta' \ell^+ \nu$		$5.0 \pm 1.3$			$2.3 \pm 0.6$
$D_s^+ + D^+$	$695.6 \pm 40.6$	$381.0 \pm 30.5$	$31.4 \pm 7.9$		
$D_s^+$ fraction ( $f_{D_s^+}$ )		0.855	0.926		0.989
$D_s^+$ signal yield	$695.6 \pm 40.6$	$325.6 \pm 26.1$	$29.1 \pm 7.3$		
$D_s^{*+} + \text{Photon bkgd.}$				$275.5 \pm 27.2$	$114.8 \pm 15.1$
$D_s^{*+}$ fraction ( $f_{D_s^{*+}}$ )				0.759	0.803
$D_s^{*+}$ signal yield				$209.2 \pm 20.6$	$92.2 \pm 12.1$
$\epsilon \mathcal{B}(\%)$	2.078	0.807	0.204	1.408	0.474
Corrected yield	$33468 \pm 1952$	$40368 \pm 3232$	$14256 \pm 3572$	$14862 \pm 1466$	$19460 \pm 2552$

There are two main sources of background:  $X$  accompanied by a fake lepton, and random  $X\ell^+$  combinations. The background due to fake leptons is estimated by using real data to measure the momentum dependent probabilities that a hadron will be misidentified as a lepton, typically 0.3% for electrons and 1.2% for muons. The hadrons in the data events are then treated as leptons and weighted by the fake probabilities to give the fake background. All background estimates and signal yields are given in Table I.

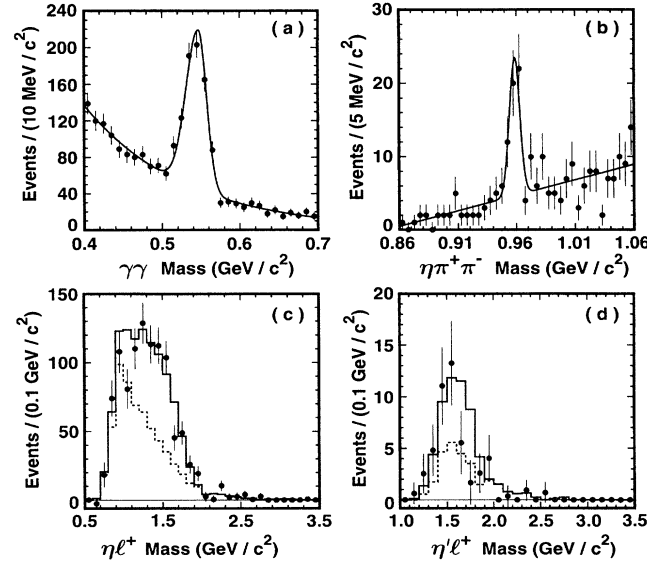


FIG. 1. The (a)  $\gamma\gamma$  and (b)  $\eta\pi^+\pi^-$  invariant mass spectra for  $D_s^+ \rightarrow \eta \ell^+ \nu$  and  $D_s^+ \rightarrow \eta' \ell^+ \nu$  candidates in the  $D_s^{*+}$  nontag analysis: The solid curve is a fit to each spectrum. (c)  $\eta\ell^+$  and (d)  $\eta'\ell^+$  are invariant mass spectra for the candidates: The points with error bars represent the number of candidates in each mass bin. The solid histogram shows the simulated signal plus the predicted background, and the dotted histogram shows the predicted background. We removed the cut on  $\eta\ell^+$  and  $\eta'\ell^+$  invariant masses discussed in the text for (c) and (d).

Random  $X\ell^+$  combinations come from  $e^+e^- \rightarrow c\bar{c}$  events in which an  $X$  produced in the fragmentation process is combined with a lepton from a semileptonic decay of the charmed hadron in the same jet, or from  $Y(4S) \rightarrow B\bar{B}$  events in which an  $X$  and a lepton produced in the decay of the  $B$  and  $\bar{B}$  mesons are combined. The background from random  $X\ell^+$  combinations is estimated using a Monte Carlo simulation which is then scaled by comparison with data. To determine the scale factor, for the case in which a fragmentation  $X$  is produced in the same jet as a charmed meson, we use a sample containing reconstructed  $D^0 \rightarrow K^-\pi^+$  decays with  $D^0$  momenta in the same range as those of our  $D_s^+$  sample. The direction of the charmed meson is close to that of the high momentum lepton in charm semileptonic decays. The yields of  $D^0$  and  $X$  mesons produced in the same hemisphere are obtained by fitting the invariant mass distributions. In data  $1.2 \pm 0.5$   $\eta$  mesons are found for every 1000 reconstructed  $D^0$  mesons, which is to be compared with  $1.7 \pm 0.1$  in the  $e^+e^- \rightarrow c\bar{c}$  Monte Carlo sample. We therefore scale the Monte Carlo estimate of the charm continuum background for  $D_s^+ \rightarrow \eta \ell^+ \nu$  by  $0.7 \pm 0.3$ . The corresponding scale factors for  $D_s^+ \rightarrow \phi \ell^+ \nu$  and  $D_s^+ \rightarrow \eta' \ell^+ \nu$  are  $1.0 \pm 0.7$  and  $0.0_{-0.0}^{+0.4}$ , respectively.

The background from random  $X\ell^+$  combinations in  $B\bar{B}$  events is estimated in a similar manner, though in this case the directions of the  $X$  and the lepton are uncorrelated. We therefore compare the number of  $X$ 's with momentum above  $1.0 \text{ GeV}/c$  in the continuum subtracted  $Y(4S)$  data with the number observed in the  $Y(4S) B\bar{B}$  Monte Carlo sample. The scale factors for  $D_s^+ \rightarrow \phi \ell^+ \nu$ ,  $D_s^+ \rightarrow \eta \ell^+ \nu$ , and  $D_s^+ \rightarrow \eta' \ell^+ \nu$  are  $1.0 \pm 0.1$ ,  $1.1 \pm 0.1$ , and  $0.3 \pm 0.2$ , respectively. The resulting backgrounds are found by scaling the Monte Carlo estimate.

There are also backgrounds from correctly reconstructed charm decays. For  $D_s^+ \rightarrow \eta \ell^+ \nu$  decay, we estimate the feed down from  $D_s^+ \rightarrow \eta' \ell^+ \nu$  by multiplying the efficiency corrected yield of the observed  $D_s^+ \rightarrow \eta' \ell^+ \nu$  decay (discussed below) by the appropriate

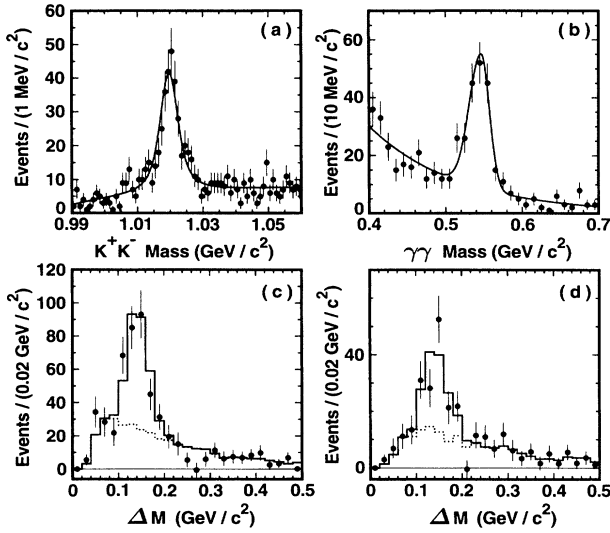


FIG. 2. The (a)  $K^+K^-$  and (b)  $\gamma\gamma$  invariant mass spectra for  $D_s^+ \rightarrow \phi\ell^+\nu$  and  $D_s^+ \rightarrow \eta\ell^+\nu$  candidates in the  $D_s^{*+}$  tag analysis: Note that a candidate photon from the  $D_s^{*+}$  is required. The solid curve is a fit to each spectrum. The spectra of the pseudomass difference  $\Delta M$  for (c)  $D_s^+ \rightarrow \phi\ell^+\nu$  and (d)  $D_s^+ \rightarrow \eta\ell^+\nu$  candidates: The points with error bars represent the number of candidates in each  $\Delta M$  bin. The solid histogram shows the simulated signal plus the predicted background, and the dotted histogram shows the predicted background. We removed the cut on  $\Delta M$  discussed in the text for (c) and (d).

efficiency and the branching fraction. The Cabibbo suppressed decay  $D^+ \rightarrow \eta\ell^+\nu$  contributes a sizable contamination to  $D_s^+ \rightarrow \eta\ell^+\nu$  in the  $D_s^{*+}$  nontag analysis. Using a measurement of the cross section ratio of  $\sigma(D^+)/\sigma(D_s^+)$  [7] and the ISGW2 model [8] for the ratio of widths,  $\Gamma(D^+ \rightarrow \eta(\eta')\ell^+\nu)/\Gamma(D_s^+ \rightarrow \eta(\eta')\ell^+\nu)$ , we estimate the fraction of the yield which is  $D_s^+$  to be  $f_{D_s^+}^\eta = 0.855 \pm 0.051$  ( $f_{D_s^+}^{\eta'} = 0.926 \pm 0.026$ ) for an  $\eta$ - $\eta'$  mixing angle of  $-15^\circ \pm 5^\circ$ .

Figures 1(c) and 1(d) show the fitted number of  $\eta$  and  $\eta'$  in each bin of  $\eta\ell^+$  and  $\eta'\ell^+$  mass, respectively. The combined background estimate is also shown, as well as the sum of the simulated signal and the combined background estimate. The simulated signal has been normalized to the number of candidates extracted from the fit to the  $\gamma\gamma$  and  $\eta\pi^+\pi^-$  invariant mass spectra. Table I gives the yields after correcting for efficiencies, the  $\phi \rightarrow K^+K^-$ ,  $\eta \rightarrow \gamma\gamma$ , and  $\eta' \rightarrow \eta\pi^+\pi^-$  branching fractions. Because of the higher identification efficiency of electrons

relative to muons, the electrons form about 75% of the total signal yield.

In the  $D_s^{*+}$  tag analysis, we look for a low energy photon from the  $D_s^{*+} \rightarrow D_s^+\gamma$  decay in the same jet as  $X$  ( $\equiv \phi$  or  $\eta$ ) and the lepton. The photon candidate must now lie in the fiducial region  $|\cos\theta| < 0.71$  and have energy greater than 0.12 GeV. To further suppress background photons from  $\pi^0$  decays, we veto any photon that has an invariant mass consistent with the  $\pi^0$  mass when combined with another photon. To select  $X\ell^+\gamma$  candidates we require that  $\Delta M \equiv M_{X\ell^+\gamma} - M_{X\ell^+}$  be between 0.1 and 0.2  $\text{GeV}/c^2$ , where  $M_{X\ell^+}$  and  $M_{X\ell^+\gamma}$  are the invariant masses of the  $X\ell^+$  and  $X\ell^+\gamma$  systems, respectively. Figures 2(a) and 2(b) show the  $K^+K^-$  and  $\gamma\gamma$  invariant mass spectra for all  $\phi\ell^+\gamma$  and  $\eta\ell^+\gamma$  combinations which pass the above selection criteria.

The backgrounds due to fake leptons, random  $X\ell^+$  combinations, and  $D_s^+ \rightarrow \eta'\ell^+\nu$  feed down are estimated by the same procedures as for the  $D_s^{*+}$  nontag analysis. The background from the combination of a true  $X\ell^+$  and a random photon is estimated using a Monte Carlo simulation, which is verified by using events containing the decay chain,  $D^{*+} \rightarrow D^0\pi^+$ , and  $D^0 \rightarrow K^-e^+\nu$ ; the  $K^-e^+$  pair has kinematics similar to that of an  $X\ell^+$  pair from  $D_s^+$  decay. We combine photons with  $K^-e^+$  pairs selected with the same criteria as for  $X\ell^+$  from  $D_s^+$  decay. In data  $21.4 \pm 1.7$   $K^-e^+\gamma$  combinations are found for every 100 reconstructed  $K^-e^+$  pairs, which is to be compared with  $22.3 \pm 0.1$  for the Monte Carlo sample. Scaling the Monte Carlo by the factor of  $0.96 \pm 0.08$ , we predict the ratio of the signal to the sum of the signal and the random photon background,  $f_{D_s^+}$ , to be  $0.759 \pm 0.030$  for  $D_s^+ \rightarrow \phi\ell^+\nu$  and  $0.803 \pm 0.031$  for  $D_s^+ \rightarrow \eta\ell^+\nu$ . Figures 2(c) and 2(d) show the fitted number of  $\phi$  and  $\eta$  in each  $\Delta M$  bin, respectively.

To obtain the effective branching ratio in the electron channel, we take into account the reduced phase space in the muon channel [9], and the efficiency loss due to final state radiation for electronic decays [10]. The results for  $\mathcal{B}(D_s^+ \rightarrow \eta e^+\nu)/\mathcal{B}(D_s^+ \rightarrow \phi e^+\nu)$  are  $1.21 \pm 0.12 \pm 0.16$  and  $1.32 \pm 0.22 \pm 0.15$  for the nontag and tag analyses, respectively. The nontag analysis is statistically almost uncorrelated with the tag analysis (21% of the nontag sample overlaps with the tag sample). The two measurements for  $\eta/\phi$  are combined with the weight for each measurement formed from the statistical and uncorrelated systematic errors. This result and the  $\eta'/\phi$  and  $\eta'/\eta$  measurements from the nontag analysis are given

TABLE II. Summary of measurements and predictions. The numbers in (parentheses) [brackets] are the ISGW2 predictions using values of the  $\eta$ - $\eta'$  mixing angle of  $(-10^\circ)$  and  $[-20^\circ]$ .

	This experiment	E653	ISGW2
$\mathcal{B}(D_s^+ \rightarrow \eta e^+\nu)/\mathcal{B}(D_s^+ \rightarrow \phi e^+\nu)$	$1.24 \pm 0.12 \pm 0.15$		(1.17)[0.77]
$\mathcal{B}(D_s^+ \rightarrow \eta' e^+\nu)/\mathcal{B}(D_s^+ \rightarrow \phi e^+\nu)$	$0.43 \pm 0.11 \pm 0.07$	$< 1.6$ at 90% C.L.	(0.50)[0.67]
$\mathcal{B}(D_s^+ \rightarrow \eta' e^+\nu)/\mathcal{B}(D_s^+ \rightarrow \eta e^+\nu)$	$0.35 \pm 0.09 \pm 0.07$		(0.43)[0.86]
$\mathcal{B}(D_s^+ \rightarrow \phi e^+\nu)/\mathcal{B}(D_s^+ \rightarrow (\eta + \eta')e^+\nu)$	$0.60 \pm 0.06 \pm 0.06$	$0.26^{+0.18}_{-0.07}$	(0.60)[0.69]

in Table II. The major contributions to the systematic error (12.1%) in  $\mathcal{B}(D_s^+ \rightarrow \eta e^+ \nu)/\mathcal{B}(D_s^+ \rightarrow \phi e^+ \nu)$  are the uncertainties in the  $D^+ \rightarrow \eta e^+ \nu$  (5.9%), fake lepton (5.9%), charm continuum backgrounds (5.2%), and uncertainties in the fit (5.8%). The systematic errors in  $\mathcal{B}(D_s^+ \rightarrow \eta' e^+ \nu)/\mathcal{B}(D_s^+ \rightarrow \phi e^+ \nu)$  and  $\mathcal{B}(D_s^+ \rightarrow \eta' e^+ \nu)/\mathcal{B}(D_s^+ \rightarrow \eta e^+ \nu)$  are dominated by the uncertainty in the charm continuum background (12.7% for  $\eta'/\phi$ , and 13.0% for  $\eta'/\eta$ ).

Using the factorization hypothesis, Kamal *et al.* predict  $\mathcal{B}(D_s^+ \rightarrow \eta' e^+ \nu)/\mathcal{B}(D_s^+ \rightarrow \eta e^+ \nu) = \mathcal{B}(D_s^+ \rightarrow \eta' \rho^+)/\mathcal{B}(D_s^+ \rightarrow \eta \rho^+)$  [11]. However, CLEO has measured  $\mathcal{B}(D_s^+ \rightarrow \eta' \rho^+)/\mathcal{B}(D_s^+ \rightarrow \eta \rho^+) = 1.20 \pm 0.35$  [12], which is in marked disagreement with our measurement,  $\mathcal{B}(D_s^+ \rightarrow \eta' e^+ \nu)/\mathcal{B}(D_s^+ \rightarrow \eta e^+ \nu) = 0.35 \pm 0.09 \pm 0.07$ .

In conclusion, we have measured  $\mathcal{B}(D_s^+ \rightarrow \eta e^+ \nu)/\mathcal{B}(D_s^+ \rightarrow \phi e^+ \nu) = 1.24 \pm 0.12 \pm 0.15$  and  $\mathcal{B}(D_s^+ \rightarrow \eta' e^+ \nu)/\mathcal{B}(D_s^+ \rightarrow \phi e^+ \nu) = 0.43 \pm 0.11 \pm 0.07$ , which agree with the predictions of ISGW2 for an  $\eta$ - $\eta'$  mixing angle of  $-10^\circ$ . Our value for the ratio of vector to pseudoscalar final states in  $D_s^+$  semileptonic decay,  $0.60 \pm 0.06 \pm 0.06$ , agrees with that observed in  $D$  semileptonic decay,  $0.56 \pm 0.06$  [1], and also with the ISGW2 model prediction. This agreement increases confidence in the evaluations of the  $D_s^+ \rightarrow \phi \pi^+$  branching ratio using models of semileptonic decays and measurements of  $\Gamma(D_s^+ \rightarrow \phi \ell^+ \nu)/\Gamma(D_s^+ \rightarrow \phi \pi^+)$  [1,2].

We gratefully acknowledge the effort of the CESR staff in providing us with excellent luminosity and running conditions. This work was supported by the National Science Foundation, the U.S. Department of Energy, the

Heisenberg Foundation, the Alexander von Humboldt Stiftung, the Natural Sciences and Engineering Research Council of Canada, and the A. P. Sloan Foundation.

---

\*Permanent address: University of Hawaii at Manoa, Honolulu, HI 96801.

- [1] Particle Data Group, L. Montanet *et al.*, Review of Particle Properties, Phys. Rev. D **50**, 1565 (1994).
- [2] J. D. Richman and P. R. Burchat, Report No. UCSB-HEP-95-08 and Stanford-HEP-95-01 [Rev. Mod. Phys. (to be published)].
- [3] E653 Collaboration, K. Kodama *et al.*, Phys. Lett. B **309**, 483 (1993).
- [4] CLEO Collaboration, Y. Kubota *et al.*, Nucl. Instrum. Methods Phys. Res., Sect. A **320**, 66 (1992).
- [5] G. C. Fox and S. Wolfram, Phys. Rev. Lett. **41**, 1581 (1978).
- [6] N. Isgur *et al.*, Phys. Rev. D **39**, 799 (1989).
- [7] CLEO Collaboration, P. Avery *et al.*, Report No. CLNS 90-992 (to be published).
- [8] D. Scora and N. Isgur, Report No. CEBAF-TH-94-14 (to be published).
- [9] J. G. Körner and G. A. Schuler, Z. Phys. C **46**, 93 (1990).
- [10] D. Atwood and W. J. Marciano, Phys. Rev. D **41**, 1736 (1990).
- [11] A. N. Kamal *et al.*, Phys. Rev. D **49**, 1330 (1994). However, using different form factor shapes, R. C. Verma *et al.*, in Z. Phys. C **65**, 255 (1995), make a prediction closer to our result.
- [12] CLEO Collaboration, P. Avery *et al.*, Phys. Rev. Lett. **68**, 1279 (1992).